Nonlinear simplified LFT modelling of an aircraft on ground

J-M. Biannic, A. Marcos, M. Jeanneau and C. Roos

***Abstract*— In this paper, a simplified nonlinear LFT model of an aircraft-on-ground is developed and compared to a full nonlinear model. The proposed simplifications are shown to be not so restrictive. The main contribution of the paper consists of an original approximation of the ground forces. Based on this approximation, which yet remains quite close to reality, some strong nonlinearities of the initial model are conveniently replaced by saturations and time-varying uncertainties. Thus, the proposed simplified model boils down to a reduced order LFT where the Δ block only contains time-varying or constant (but uncertain) parameters on the one hand, and saturation-type non-linearities on the other hand. Such a model is then very useful for applying modern analysis and synthesis techniques.**

Keywords : Aircraft-on-ground dynamics, LFT modelling, nonlinear systems, saturations.

I. INTRODUCTION

Over the past twenty years fly-by-wire systems have been widely spread on board transport aircraft, allowing for increased piloting comfort, flight domain protections, automatic flight navigation, automatic landing systems, and many others. All these automated functions either help pilots accomplishing their duties, or significantly increase on-board safety. However the ground motion of commercial aircraft is still achieved by manual control of rudder deflection, engines running speed, wheels brakes and nose-wheel steering system. Yet in order to reduce the congestion of many airports while increasing safety, there is a real need to develop new control systems improving and facilitating aircraft on-ground handling qualities [7]. Consequently, simplified (control-oriented) aircraft models including on-ground dynamics are required. Ground forces affecting aircraft have to be considered in addition to aerodynamic forces. The relative complexity of these ground forces make the modelling task challenging. Highly nonlinear effects are to be considered and many uncertain parameters influence the various phenomena considered. In this paper linear parameter varying (LPV) and linear fractional transformation (LFT) modeling is used together with a novel force identification approach based on nonlinear dynamic inversion (NDI) theory [8] to obtain such simplified model while preserving a sufficient precision level. As a result the simplified LPV-LFT model obtained is valid not only for control design purposes but also for validation tasks.

II. A SHORT DESCRIPTION OF THE FULL MODEL

The full aircraft model is derived from the general nonlinear state-space equations as summarized below :

$$\begin{bmatrix} \dot{V} \\ \dot{\Omega} \end{bmatrix} = \begin{bmatrix} \frac{F}{m} - \Omega \wedge V \\ I^{-1}(M - \Omega \wedge (I.\Omega)) \end{bmatrix} \quad (1)$$

J-M. Biannic and C. Roos are with the Department of Flight Control Systems and Dynamics of ONERA, Toulouse, France biannic@onera.fr

A. Marcos is with the Advanced Projects Division of Deimos Space, Madrid, Spain andres.marcos@deimos-space.com

M. Jeanneau is with the Stability and Control Department of AIRBUS, Toulouse, France matthieu.jeanneau@airbus.com

with the following standard notations :

$V = [V_x, V_y, V_z]^T$	velocity vector at *c.g.*
$\Omega = [p, q, r]^T$	ang. velocity vector about *c.g.*
$F = [F_x, F_y, F_z]^T$	Total external force vector
$M = [M_r, M_p, M_q]^T$	Total external torque vector
I	Inertia tensor
m	mass of the aircraft.

The main forces and moments acting on the aircraft on ground are due to the aerodynamic effects, gravity, engine thrust and forces related to interactions with the ground. Aerodynamic effects and engine thrust are modelled via neural networks [9]. But, for this specific application, the most important part of the model comes from forces which are induced by the contact between the tyres and the ground. In this paper, a special interest is dedicated to lateral forces which appear when the velocity is no longer oriented in the plane of the wheel, e.g. the wheel slips on the ground. This sideslip can be compared to a lateral velocity component generating deformations in the tyre and friction forces. This force is thus presented as a nonlinear function of the sideslip angle, but it also depends on many other parameters such as the vertical load, the grip on the ground (dry, wet,icy) and the velocity of the aircraft. Here, a macroscopic nonlinear model is used which combines various elements from [2], [1], [5]. More technical details are given in the next section.

III. SIMPLIFYING THE ON-GROUND MODEL

In order to simplify the general equations and to obtain a tractable model for control law development but also for robustness analysis tasks, the following assumptions have been considered :

- *(A1)* No roll and pitch variations ($p = 0$, $q = 0$)
- *(A2)* Bicycle hypothesis
- *(A3)* Simplified expressions for aerodynamic efforts
- *(A4)* Small angle and low speed (< 150 knots)

The first assumption is quite standard in the study of the on-ground behavior. It will considerably simplify the equations while preserving the quality of the model for a large class of manœuvers. The main manœuvers for which this approximation might not be well suited are those requiring a severe braking which induces a significant pitch movement.

The bicycle hypothesis consists in a simplification of the main landing gear which is reduced to a single tyre. This approximation is quite useful since it greatly simplifies the expressions of local sideslip angles from which friction forces are evaluated. As long as specific manœuvers, such as differential braking for example, are not to be studied, it will be shown that this approximation is not restrictive.

The third assumption, which consists in limiting the complexity of the aerodynamic coefficients will be further detailed below. It is often used in the description of flight

dynamics and fully justified here since both the speed and altitude range are quite limited –indeed, this limited range also validates the last assumption. Moreover, as the speed decreases, then the aerodynamic efforts become negligible in comparison with ground forces.

Thanks to assumption *(A1)*, the general equations (1) are reduced to a 3 Degree-of-Freedom (DoF) on-ground model :

$$\left\{ \begin{array}{l} \dot{r} = \frac{M_r}{I_{zz}} \\ \dot{V}_y = \frac{F_y}{m} - rV_x \\ \dot{V}_x = \frac{F_x}{m} + rV_y \end{array} \right. \tag{2}$$

where the forces F_x, F_y and moment M_r can be split up into aerodynamic, gravity, thrust and ground parts :

$$\left\{ \begin{array}{l} F_x = -\frac{1}{2}\rho SV^2(C_x c_\alpha + C_z s_\alpha) - g s_\theta + \sum Tn + F_{x_g} \\ F_y = \frac{1}{2}\rho SV^2 C_y + F_{y_g} \\ M_r = \frac{1}{2}\rho ScV^2 C_n + M_{r_g} \end{array} \right. \tag{3}$$

Using assumptions *(A3)* and *(A4)*, the aerodynamic coefficients are simplified as follows :

$$\left\{ \begin{array}{l} (C_x c_\alpha + C_z s_\alpha) = C_{x_0} \\ C_y = C_{y_\beta}\beta_a + C_{y_\delta}\delta_r + C_{y_r}\frac{rc}{V} \\ C_n = C_{n_\beta}\beta_a + C_{n_\delta}\delta_r + C_{n_r}\frac{rc}{V} \end{array} \right. \tag{4}$$

where C_{x_0} is a constant and the aerodynamic sideslip angle β_a can be approximated by (W_y denoting the lateral wind) :

$$\beta_a = \frac{V_y}{V} + \frac{W_y}{V} \tag{5}$$

A. On-Ground forces simplification

Let us now detail the forces generated by the tyres friction with the ground. Using the bicycle hypothesis, these forces can be split up into nose-wheel (NW) and main-landing-gear (MG) components:

$$\left\{ \begin{array}{l} F_{x_g} = F_{x_{NW}} + F_{x_{MG}} = -\theta_{NW} F_{y_{NW}} + F_{x_{MG}} \\ F_{y_g} = F_{y_{NW}} + F_{y_{MG}} \end{array} \right. \tag{6}$$

where θ_{NW} corresponds to the nose-wheel angle (which is controlled by the steering system) and the two F_{y_g} components depend respectively on the nose-wheel and main landing gear sideslip angles which, thanks to assumption *(A2)*, can be expressed as follows :

$$\left\{ \begin{array}{l} \beta_{NW} = arctan \underbrace{\left(\frac{V_y + L_{NW}.r}{V_x} \right)}_{\tilde{\beta}_{NW}} - \theta_{NW} \\ \beta_{MG} = arctan \underbrace{\left(\frac{V_y - L_{MG}.r}{V_x} \right)}_{\tilde{\beta}_{MG}} \end{array} \right. \tag{7}$$

L_{NW}, L_{MG} denote distances between the center of gravity and nose-wheel or main gear, along the longitudinal axis of the aircraft.

Finally, the moment generated by ground forces is easily obtained from the two components of F_{y_g} :

$$M_{r_g} = M_{r_{NW}} + M_{r_{MG}} \tag{8}$$

with :

$$\left\{ \begin{array}{l} M_{r_{NW}} = F_{y_{NW}}(\beta_{NW}) L_{NW} \\ M_{r_{MG}} = -F_{y_{MG}}(\beta_{MG}) L_{MG} \end{array} \right. \tag{9}$$

IV. LATERAL LPV MODEL WITH APPROXIMATED FORCES

In this section we focus on the development of an LPV model for the lateral motion, which includes approximating the ground forces using a novel identification method based on NDI theory.

A. Lateral LPV model

Combining the previous equations, a 2-DoF lateral LPV model with time-varying vector $\theta = [V \;\; V_x]^T$ is obtained :

$$\left\{ \begin{array}{l} \begin{bmatrix} \dot{r} \\ \dot{V}_y \end{bmatrix} = A_a(\theta) \begin{bmatrix} r \\ V_y \end{bmatrix} + B_a(\theta) \begin{bmatrix} W_y \\ \delta_r \end{bmatrix} + B_{tyres} \begin{bmatrix} F_{y_{NW}} \\ F_{y_{MG}} \end{bmatrix} \\ \begin{bmatrix} \tilde{\beta}_{NW} \\ \beta_{MG} \end{bmatrix} = C_\beta(\theta) \begin{bmatrix} r \\ V_y \end{bmatrix} \end{array} \right. \tag{10}$$

where :

$$A_a = \begin{bmatrix} 0 & 0 \\ -V_x & 0 \end{bmatrix} + \frac{\rho SV}{2} \begin{bmatrix} \frac{c^2 C_{n_r}}{I_{zz}} & \frac{cC_{n_\beta}}{I_{zz}} \\ \frac{cC_{y_r}}{m} & \frac{C_{y_\beta}}{m} \end{bmatrix} \tag{11}$$

$$B_a = \frac{\rho SV}{2} \begin{bmatrix} \frac{cC_{n_\beta}}{I_{zz}} & \frac{cVC_{n_\delta}}{I_{zz}} \\ \frac{C_{y_\beta}}{m} & \frac{VC_{y_\delta}}{m} \end{bmatrix} \tag{12}$$

$$B_{tyres} = \begin{bmatrix} \frac{L_{NW}}{I_{zz}} & -\frac{L_{MG}}{I_{zz}} \\ \frac{1}{m} & \frac{1}{m} \end{bmatrix} \tag{13}$$

$$C_\beta = \frac{1}{V_x} \begin{bmatrix} L_{NW} & 1 \\ -L_{MG} & 1 \end{bmatrix} \tag{14}$$

Note that the inputs to B_{tyres} are the components of the nonlinear lateral ground forces F_{y_g}. On-line measurement of these forces is not a trivial task, therefore it is required to perform some type of approximation or identification.

B. Nonlinear ground forces approximation

For small angles, almost linear variations with respect to local sideslip angles are expected for F_{y_g} allowing to introduce some constant terms $G_{y_{NW}}$ and $G_{y_{NW}}$, referred to as cornering gains :

$$\left\{ \begin{array}{l} F_{y_{NW}}(\beta_{NW}) \approx G_{y_{NW}}.\beta_{NW} \\ F_{y_{MG}}(\beta_{MG}) \approx G_{y_{MG}}.\beta_{MG} \end{array} \right. \tag{15}$$

Generalizing this cornering gains notion to large sideslip angles, a standard nonlinear model is described by :

$$\left\{ \begin{array}{l} F_{y_{NW}}(\beta_{NW}) = G_{y_{NW}}.\beta_{NW}.\frac{1}{1+\gamma_{NW}^2} \\ F_{y_{MG}}(\beta_{MG}) = G_{y_{MG}}.\beta_{MG}.\frac{1}{1+\gamma_{MG}^2} \end{array} \right. \tag{16}$$

with :

$$\gamma_{NW} = \frac{\beta_{NW}}{\beta_{NW_{opt}}} \;\; , \;\; \gamma_{MG} = \frac{\beta_{MG}}{\beta_{MG_{opt}}} \tag{17}$$

where $\beta_{NW_{OPT}}$ and $\beta_{MG_{OPT}}$ correspond to optimal sideslip angles for which maximum lateral forces are reached.

Theoretically, the values of the cornering gains could be considered as specific constant characteristics of the tyres. Reality is unfortunately much more complex and the determination of these gains is not that simple. In fact they will not only depend on the sideslip angles (when the latter become too large), but also on the vertical loads. Furthermore, the runway state (quality of the surface and

weather conditions: dry, wet, icy) will also induce large variations on the optimum angles $\beta_{NW_{OPT}}$ and $\beta_{MG_{OPT}}$.

In the full order nonlinear model these variations are taken into account by adding to equations (16) and (17) some nonlinear functions identified from ground tests by manufacturers. Consequently, equation (16) is represented now as (the indexes $_{NW}$ and $_{MG}$ have been omitted to alleviate notation) :

$$F_y = G_y(F_z)\frac{\beta}{1+\left(\frac{\beta}{\beta_{OPT}(\lambda_{rwy})}\right)^2} \tag{18}$$

To cover all these possible variations while limiting the complexity of the model, a first approximation can be proposed which considers the cornering gains as uncertain, possibly time-varying, parameters. Moreover, a scaling factor λ_{rwy} (already shown above) is added to adapt the optimum angles as a function of the runway state. Thus, the nonlinear lateral forces in (18) could be approximated by :

$$\begin{aligned} F_{y_{LPV}} &= (1+\delta_{G_y}(t)).G_{y_{nom}}.\frac{\beta}{1+\left(\frac{\beta}{\lambda_{rwy}.\beta_{OPT}}\right)^2} \\ &= (1+\delta_{G_y}(t)).F_{y_{nom}}(\beta,\lambda_{rwy}) \end{aligned} \tag{19}$$

where the time-varying uncertain parameter $\delta_{G_y}(t)$ will typically satisfy the following bounds :

$$-0.4 \leq \delta_{G_y}(t) \leq 0.4 \tag{20}$$

which means that the precision level on the cornering gains is rather poor (40%).

C. Ground force NDI identification procedure

An alternative approach to the approximation given by equation (19) is to calculate $F_{y_{LPV}}$ using an off-line identification approach followed by a function fitting. Such an approach is proposed now based on NDI theory and using the full nonlinear plant as the reference input.

Let us denote $\hat{F}_{y_g}$ the vector of identified forces and introduce the following notations :

$x_{NL} = [r_{NL}\ V_{y_{NL}}]^T$	state of nonlinear model
$x_{LPV} = [r_{LPV}\ V_{y_{LPV}}]^T$	state of LPV model
$u_a = [W_y\ \delta_r]^T$	aerodynamic inputs

Remarking that B_{tyres} is a nonsingular square matrix, the dynamic equations in (10) may be inverted as follows :

$$\hat{F}_{y_g} = B_{tyres}^{-1}\left(\dot{x}_{LPV} - A_a(\theta)x_{LPV} - B_a(\theta)u_a\right) \tag{21}$$

which shows that, at each time, the derivative signal $\dot{x}_{LPV}$ can be fully controlled by an appropriate choice of $\hat{F}_{y_g}$. Indeed, $\dot{x}_{LPV}$ represents the desired signal which drives the identification procedure. The goal of the identification procedure is then to have $\dot{x}_{LPV} = \dot{x}_d$ equal to zero, except maybe during transients. This can be achieved using a proportional (like in classical control) identification law :

$$\dot{x}_d = \lambda(x_{NL} - x_{LPV}) \tag{22}$$

It is easily seen that, for any continuous trajectory, and sufficiently high values of λ, the states of the LPV model remain as close as desired to those of the full nonlinear system provided that $F_{y_{LPV}} = \hat{F}_{y_g}$.

D. NDI force identification results

The validity of the proposed identification procedure and the approximated LPV model can be tested for several manœuvers designed to evaluate both the ground and the aerodynamic parts of the model. For each manœuver, three runway state conditions are tested: dry, wet and icy. Moreover, uncertainties ($\pm 40\%$) are applied to the cornering gains as in equation (20).

During each simulation, ground forces are identified so that the outputs of the LPV model match those of the full nonlinear system. A lot of information can be read-off from plotting the identified forces $\hat{F}_{y_{NW}}$ and $\hat{F}_{y_{MG}}$ versus β_{NW} and β_{MG} respectively (see figure 1). For example, the proposed model is graphically validated if these plots are close to the graphs from the two nonlinear functions given by equation (18).

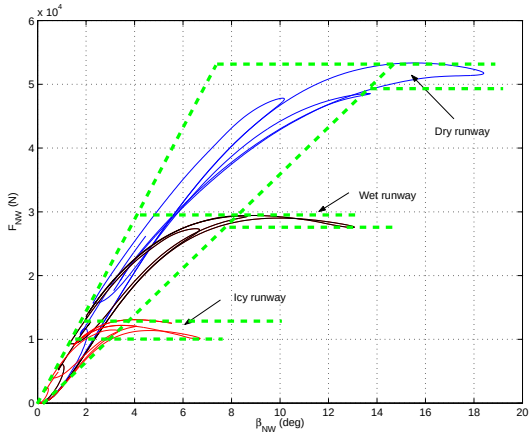

Fig. 1. $\hat{F}_{y_{NW}}$ versus β_{NW}

A short examination of figure 1 seems to reveal *a priori* a problem with the model, since the plots cannot be approximated obviously by single-valued functions (i.e. they do not depend alone on the sideslip angles). This is not surprising since many simplifications have been made and now the ground forces are used so that the proposed model behaves exactly as the full nonlinear system. Nevertheless, note that the identified lateral force can be expressed as (indexes have been omitted again) :

$$\hat{F}_y(\beta) = F_{y_{nom}}(\beta) + \hat{\Delta}(x) \tag{23}$$

where $\hat{\Delta}$ stands for a virtual (in a sense that it has no direct physical meaning) nonlinear operator which may depend on the whole state vector of the system.

Recall from equations (19) and (20) that F_y itself is affected by a high level (40%) of uncertainty. Consequently, for a given runway state, as long as the dispersion $\hat{\Delta}(x)$ does not exceed 40% of the nominal value, then the model has passed the validation test.

Let us then observe the dashed lines of figure 1 more closely now. These lines (starting from the origin) correspond to maximum and minimum values of the estimated forces. Using the linear approximations, extremal values of $\hat{G}_{NW}$ and $\hat{G}_{MG}$ can be immediately deduced and consequently $G_{y_{nom}}$ (see table I which also indicates the relative errors).

	min	max	error (%)
$\hat{G}_{NW}(N/rad)$	$1.1\ 10^5$	$2.5\ 10^5$	38.9
$\hat{G}_{MG}(N/rad)$	$4\ 10^5$	$5\ 10^5$	11

TABLE I
EXTREMAL VALUES OF THE CORNERING GAINS

Using equations (19), a natural approach to complete the description of the forces would be to identify the optimum values β_{OPT} (easily achieved using figure 1). Yet, this approach will generate complex models which might not be well suited for robustness analysis or synthesis techniques. Therefore, let us now ask the following question :

Is it really useful to develop an accurate model for large sideslip angles, beyond β_{OPT} ?

Obviously, at least for design-oriented models, the answer is *no*, because the control system is supposed to guarantee that sideslip angles will never go beyond that limit. Consequently, as is suggested by the horizontal dashed-lines in figure 1, the lateral forces may be more efficiently approximated by the following fit :

$$\begin{cases} F_{y_{NW}} \approx sat_{L_{NW}(\lambda_{rwy})}\left(\hat{G}_{NW}(t).\beta_{NW}\right) \\ F_{y_{MG}} \approx sat_{L_{MG}(\lambda_{rwy})}\left(\hat{G}_{MG}(t).\beta_{MG}\right) \end{cases} \tag{24}$$

where $L_{NW}(\lambda_{rwy})$, $L_{MG}(\lambda_{rwy})$ denote the maximum values of the lateral forces. As illustrated in figure 1, these values clearly depend on the runway state λ_{rwy} but, as is also seen in the plot, it is straight forward to introduce additional uncertainty level on $L_{NW}(\lambda_{rwy})$ to reduce the range of variations on $\hat{G}_{NW}$.

V. LONGITUDINAL LPV MODEL

Similarly as above, a longitudinal LPV model is obtained with $\theta_2 = [V \ \ V_y]^T$ (we omit the details of the simplifications used for reason of space) :

$$[\,\dot{V}_x\,] = A_b(\theta_2)\begin{bmatrix} r \\ V_x \end{bmatrix} + B_b(\theta_2)\begin{bmatrix} W_x \\ Tn_R \\ Tn_L \end{bmatrix} + B_{b_{tyres}}\begin{bmatrix} F_{x_{NW}} \\ F_{x_{MG}} \end{bmatrix} \tag{25}$$

and the system matrices are given by :

$$A_b = [\,V_y \quad 0\,] - [\,gc_0 \quad \tfrac{\rho S V C_{x_0}}{2m}\,] \tag{26}$$

$$B_b = \tfrac{1}{m}\,[\,-\tfrac{\rho S V}{2}C_{x_0} \quad 1 \quad 1\,]; \ \ B_{b_{tyres}} = \tfrac{1}{m}\,[-1 \quad 2\,] \tag{27}$$

where c_0, C_{x_0} are constants obtained through simulation tests; coupling terms with the lateral model are introduced $(V_y r - gc_0 r)$, and the longitudinal ground forces are approximated following equations (6) and (24) as :

$$\begin{cases} F_{x_{NW}} = -\theta_{NW} F_{y_{NW}} \\ F_{x_{MG}} \approx sat_{L_{xMG}}\left(-4\hat{G}_{xMG}.V_x\right) \end{cases} \tag{28}$$

VI. LFT MODELLING

All the necessary ingredients have now been introduced to complete the LFT modelling of the aircraft-on-ground. This task can be easily performed thanks to the new version of the LFR Toolbox (v2.0) [10] which can be downloaded from [11] and also with the help of additional Simulink-based tools [3] (see also [4] for a more detailed description of the tools).

A. Main LPV block

From equations (10)-(14) and (25)-(28), putting the LPV parts of the proposed model into an LFT-LPV format (with $\theta_{LPV} = [V \ \ V_x \ \ V_y]^T$) is rather straightforward.

First, two LFT realization methods are evaluated using only the lateral LPV model. The first method is a standard numerical approach (using for example *LFRT/abcd2lfr.m*) followed by a reduction step (*LFRT/minlfr.m*). The parameters of this LFT are: V_{x_n} (normalized version of V_x), V_n (normalized version of V), δ_{C_n} (LTI multiplicative uncertainty on C_n), δ_{C_y} (LTI multiplicative uncertainty on C_y).

The second method is based on a symbolic tree decomposition algorithm [6] (*LFRT/symtreed.m*) which can be applied on polynomial matrices in symbolic form (see also [12]). Therefore, following a general method proposed in [13], V, V_x, $invV_x$, δ_{C_n}, δ_{C_y} are now defined as symbolic variables.

Remark: *It should be emphasized here that $invV_x$ is first considered as an independent variable. Thus, the rational expression is converted into a polynomial one. Note also at this stage that normalization is no longer necessary and even has to be avoided! This operation would indeed destroy the factorized structure of the polynomial matrix which is exploited by the algorithm to generate a low-order LFT.*

Once a reduced-order symbolic LFT is obtained, normalization of V and V_x is performed and $invV_x$ is defined as the inverse of V_x. These operations are easily achieved with the help of the overloaded *LFRT/eval.m* function.

The sizes of the lateral LFTs obtained are reported in table II. The symbolic approach is obviously more powerful since it provides a reduced-size LFT.

	V_n	V_{x_n}	δ_{C_n}	δ_{C_r}	size of Δ_1
method 1	4	3	2	2	11
method 2	3	3	1	1	8

TABLE II
Δ-BLOCK SIZES FOR THE LATERAL LPV PART OF THE MODEL

Applying the second method to the longitudinal model (with additional symbolic parameters for V_y and uncertainties in C_x and thrust) and combining with the above lateral LFT model the full motion LFT model is obtained.

	V_n	V_{x_n}	V_{y_n}	δ_{C_n}	δ_{C_r}	δ_{C_x}	δ_{Tn}	total
long	1	0	1	0	0	1	1	4
full	3	4	1	1	1	1	1	12

TABLE III
Δ-BLOCK SIZES FOR THE LONGITUDINAL AND FULL LPV MODELS

Noting that for on-ground manœuvers the x-component of the speed V_x is the driving component of the on-ground speed V, it is then acceptable to assume $V \approx V_x$. This simplification will reduce further the final full motion LFT size when applied to the LPV models, joined before the LFT transformation, down to $\Delta_{full} = 11$ (with the same repetitions as in Table III except $V_n = 0$ and $V_{x_n} = 6$).

B. Other nonlinear and LTV elements

The next step in the LFT modelling procedure is now to find LFT models for the ground forces and for the *atan* function which is used in the computation of β_{NW}.

LFT models for $F_{x_{MG}}$, $F_{y_{NW}}$ and $F_{y_{MG}}$ are readily obtained from equations (28) and (24), where $\hat{G}_{xMG}$, $\hat{G}_{NW}$ and $\hat{G}_{MG}$ are replaced by :

$$\begin{array}{l} \hat{G}_{xMG} \leftarrow (1+\delta_{G_{xMG}}(t))\hat{G}_{xMG_0} \\ \hat{G}_{NW} \leftarrow (1+\delta_{G_{NW}}(t))\hat{G}_{NW_0} \\ \hat{G}_{MG} \leftarrow (1+\delta_{G_{MG}}(t))\hat{G}_{MG_0} \end{array} \tag{29}$$

Using *LFRT/lfr.m*, the saturations ($sat_{L_{xMG}}$, $sat_{L_{NW}}(.)$, $sat_{L_{MG}}(.)$) and time-varying uncertainties ($\delta_{G_{xMG}}(t)$, $\delta_{G_{NW}}(t)$, $\delta_{G_{MG}}(t)$) are first defined as elementary siso LFR objects :

```
>> sat_xMG = lfr('sat_xMG','nlms',1);
>> sat_NW = lfr('sat_NW','nlms',1);
>> sat_MG = lfr('sat_MG','nlms',1);
>> delta_xMG = lfr('delta_xMG','ltv',1)
>> delta_NW = lfr('delta_NW','ltv',1)
>> delta_MG = lfr('delta_MG','ltv',1)
```

then, the equations (28) and (24) are simply translated as :

```
>> F_xMG = sat_xMG*(G_xMG0*(1+delta_xMG))
>> F_NW = sat_NW*(G_NW0*(1+delta_NW))
>> F_MG = sat_MG*(G_MG0*(1+delta_MG))
```

Finally, as is clear from equations (7), there remains to approximate the trigonometric *atan* function used in the computation of β_{NW}. To cover all cases, the approximation should be valid for $|\tilde{\beta}_{NW}| \leq 1.2$ which corresponds to an output argument equal to $50\ deg$. Such an approximation (with very good precision level $< 5\%$) can be achieved by a simple piecewise affine function :

$$\begin{array}{l} |\alpha| \leq 0.4 \ \rightarrow \ f(\alpha) = \alpha \\ |\alpha| \geq 0.4 \ \rightarrow \ f(\alpha) = \frac{2}{3}\alpha + \frac{2}{15} sign(\alpha) \end{array} \tag{30}$$

which may be conveniently rewritten as follows :

$$f(\alpha) = \frac{2}{3}\alpha + \frac{2}{15}\mathbf{sat}\left(\frac{\alpha}{0.4}\right) \tag{31}$$

where $\mathbf{sat}(.)$ here denotes a normalized saturation nonlinearity. Then, the *atan* function may now be easily described by a simple LFT object whose nonlinear Δ-block is a single saturation operator.

C. Computing the interconnection

The last phase of LFT modelling consists in connecting the above components together as illustrated by figure 2. It is well-known that the interconnection of LFTs is indeed an LFT itself.

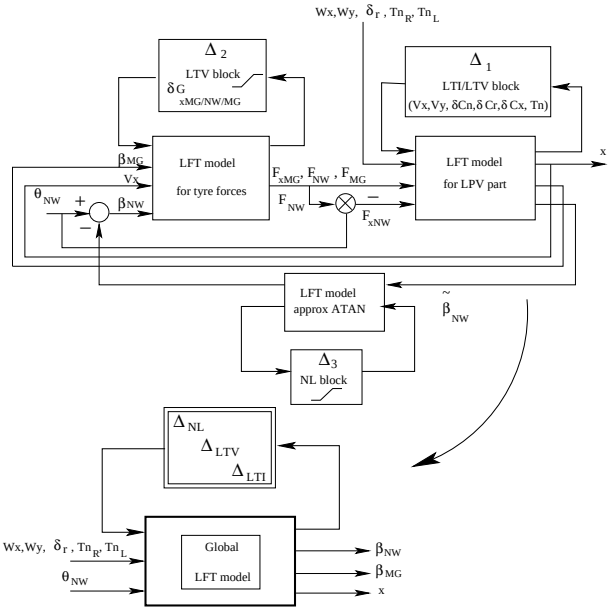

Fig. 2. Interconnection of LFTs

This step can be performed quite easily in a Simulink environment with the help of new tools [3], [4] which provide (via a specific library) a simple interface between the new version of LFR Toolbox [11] and Simulink. Using these tools, the interconnection of LFTs is simply drawn (as it appears on figure 2, but without the Δ-blocks) and saved in a Simulink file. Let us name it 'LFRslk.mdl'. Then, using a specific function *LFRT/slk/slk2lfr.m* the global LFT is readily obtained as follows :

```
>> sysLFR = slk2lfr('LFRslk');
```

This global LFT object has only three states and a 18×18 diagonal Δ-block which is structured as follows :

$$\Delta = diag(\Delta_{NL}, \Delta_{LTV}, \Delta_{LTI}) \tag{32}$$

with :

$$\begin{array}{l} \Delta_{NL} = diag\left(\mathbf{sat}_{atan}, \mathbf{sat}_{xMG}, \mathbf{sat}_{NW}, \mathbf{sat}_{MG}\right) \\ \Delta_{LTV} = diag\left(\delta_{V_x}(t).I_6\,,\ \delta_{V_y}(t)\,,\ \delta_{G_{xMG}}(t)\,, \ldots \right. \\ \qquad \left. \delta_{G_{NW}}(t)\,,\ \delta_{G_{MG}}(t)\right) \\ \Delta_{LTI} = diag\left(\delta_{C_n}, \delta_{C_y}, \delta_{C_x}, \delta_{Tn}\right) \end{array} \tag{33}$$

VII. TIME SIMULATION RESULTS

Let us now compare the outputs of our simplified LFT model with those of the full nonlinear system.

In order to evaluate both the aerodynamic and ground models, two types of manœuvers have been considered, one low-speed and the other high-speed:

- *Manœuver 1*: 40^o tiller step at T_0
- *Manœuver 4*: Full acceleration until $150\,kts$ then $\pm 5^o$ doublet in pedals followed by $\pm 2^o$ doublet in tiller

The first manœuver is applied for dry and wet runways and the second under icy conditions, figure 3, 4 and 5 respectively. The time responses are for the three states used in the simplified model (V_x, V_y, r) plus the calculated sideslip angle for the nose-wheel, β_{NW}. The full nonlinear responses are given by a (black) solid line and those for the LFT-LPV model by a (red) dashed line.

A. Low-speed manœuvers

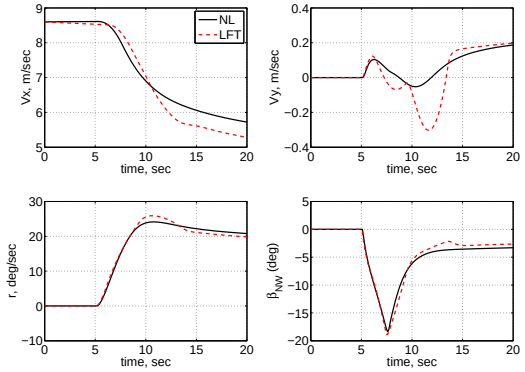

Fig. 3. Manœuver 1 : Nominal runway

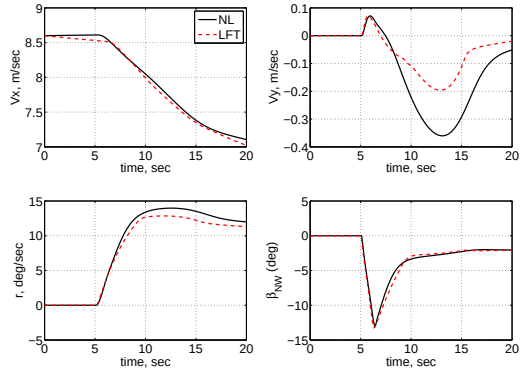

Fig. 4. Manœuver 1 : Wet runway

B. High-speed maœeuver

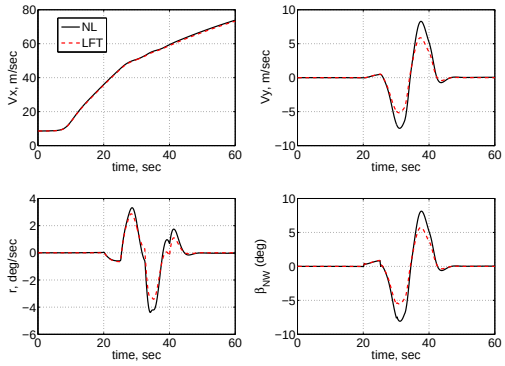

Fig. 5. Manœuver 4 : Icy runway

In all cases, it appears that the simplified LFT model performs very well. This is especially true if we focus on the yaw rate outputs (r). Furthermore, it is also observed that the assumption that the ground speed V can be approximated by its x-component V_x is valid (note, the magnitude of V_y w.r.t that of V_x).

This means that the proposed LFT model is perfectly well-suited for the development of multivariable on-ground control laws using rudder deflection, nose-wheel and differential thrust for lateral/directional control, and symmetric thrust for longitudinal control. Furthermore, its LFT-LPV nature (which includes time-varying and nonlinear blocks) facilitates the analysis of the resulting closed loops using linear and nonlinear analysis techniques, e.g. μ-worst case, IQCs, ...

VIII. CONCLUSION

In this paper a complete methodology has been described to develop a simple full-motion LFT model of an aircraft on ground. Interestingly, despite its simplicity, the proposed model performs very well on a large operating domain. It will then be very useful not only for the development of new on-ground control systems (as those proposed in [14]) but also for application of robust and nonlinear analysis techniques. Future work will be devoted to such advanced synthesis and analysis tasks.

IX. ACKNOWLEDGMENT

We gladly acknowledge the help of Dr. Declan Bates and Prof. Ian Postlethwaite from Leicester University, U.K., in funding a visit of the second author to ONERA while he was a Post-Doctoral fellow at Leicester University.

REFERENCES

[1] AGARDograph 333. Enhancement of aircraft ground handling simulation capability. In *AGARD-AG-333*, PA, 1998.

[2] E. Bakker, L. Nyborg, and H.B. Pacejka. Tyre modeling for use in vehicule dynamic studies. In *SAE paper 870421 - SAE Inc. Warrendale*, PA, 1987.

[3] J-M. Biannic and C. Döll. Simulink handling of LFR objects v1.0. Free Web publication *http://www.cert.fr/dcsd/idco/perso/Biannic/*, February, 2006.

[4] J-M. Biannic, C. Döll, and J-F. Magni. Simulink-based tools for creating and simulating interconnected LFR objects. submitted to IEEE-CCA-CACSD Conference, 2006.

[5] J. Clot and al. Systèmes d'alarme et de sécurité active pour la conduite automobile. Technical Note Ref. 98441 - LAAS-CNRS, 1998.

[6] J.C. Cockburn and B.G.Morton. Linear fractional representations of uncertain systems. *Automatica*, 33(7):1263–1271, 1997.

[7] J. Duprez, F. Mora-Camino, and F. Villaume. Aircraft-on-ground lateral control for low speed manœuvers. In *16th IFAC symposium on automatic control in aerospace*, St. Petersburg, Russia, June 2004.

[8] Enns, D., Bugajski, D., Hendrick, R., and Stein, G. Dynamic Inversion: an evolving methodology for flight control design. *International Journal of Control*, 59(1):71–91, 1994.

[9] F.Lavergne, F.Mora Camino, F.Villaume, and M.Jeanneau. Neural networks contribution to modeling for flight control. In *World Aviation Congress (WAC)*, Reno, USA, November 2004.

[10] S. Hecker, A. Varga, and J-F. Magni. Enhanced LFR Toolbox for MATLAB. In *IEEE International symposium on computer aided control system design*, Taipei, Taiwan, September 2004.

[11] J-F. Magni. Linear Fractional Representation Toolbox (version 2.0) for use with Matlab. Free Web publication *http://www.cert.fr/dcsd/idco/perso/Magni/*, 2006.

[12] A. Marcos, D. G. Bates, and I. Postlethwaite. A Multivariate Polynomial Matrix Order Reduction Algorithm for Linear Fractional Transformation Modelling. In *IFAC World Congress on Automatic Control*, Pragues, July 2005.

[13] A. Marcos, D. G. Bates, and I. Postlethwaite. Exact Nonlinear Modelling using Symbolic Linear Fractional Transformations. In *IFAC World Congress on Automatic Control*, Pragues, July 2005.

[14] C. Roos and J-M. Biannic. Aircraft-on-ground lateral control by an adaptive LFT-based anti-windup approach. submitted to IEEE-CCA-CACSD Conference, 2006.